

Higgs pair production in the MSSM with explicit CP violation

D. A. Demir ^a

^aThe Abdus Salam International Center for Theoretical Physics, I-34100, Trieste, Italy

In the minimal supersymmetric standard model with explicit CP violation, associated production of the lightest Higgs boson with heavier ones is analyzed. Due to explicit CP violation, the Higgs bosons are no longer CP eigenstates so that both of the heavy Higgs bosons contribute to the process. While the radiative corrections in the Higgs sector turn out to be quite important, the vertex radiative corrections remain small as in the CP conserving theory.

1. Introduction

The Lagrangian of the minimal supersymmetric standard model (MSSM) consists of various soft masses as well as the μ parameter coming from the superpotential [1]. In principle, gaugino masses, trilinear couplings, Higgs bilinear coupling and the μ parameter can be complex; however, not all these phases are physical [2]. Indeed, with the global symmetries of the MSSM Lagrangian, the physical phases could be reduced to those of the CKM matrix, trilinear couplings A_f , and the μ parameter [2,3].

Recently, the supersymmetric CP phases $\gamma_\mu \equiv \text{Arg}\{\mu\}$ and $\gamma_{A_f} \equiv \text{Arg}\{A_f\}$ have gotten much interest in Higgs phenomenology [4–6], FCNC processes [7], and electroweak baryogenesis [8]. Here we discuss the effects of these supersymmetric CP phases on the associated Higgs production by studying $e^+e^- \rightarrow H_{CP\ even}H_{CP\ odd}$ scattering. This process was already discussed in [9] in the CP-conserving MSSM with one-loop accuracy, and the radiative corrections were found to be at most $\sim 5\%$. We analyze the same process in the CP-violating MSSM by including the radiative corrections in the Higgs sector as well as $ZH_{CP\ even}H_{CP\ odd}$ vertex, where photon contribution is neglected as it is much smaller. Results agree with [9] in that the vertex corrections are quite small; however, radiative corrections in the Higgs sector are important. Below, in accordance with EDM [2,10] and cosmological constraints [11], γ_μ will be set to zero in course of the analysis whereas $\gamma_A \equiv \gamma_{A_t}$ will be taken as free.

2. $e^+e^- \rightarrow H_{CP\ even}H_{CP\ odd}$ Scattering

The supersymmetric CP phases γ_A and γ_μ show up in sfermion, chargino and neutralino mass matrices so that the processes involving these particles as well as their loop effects depend on these phases explicitly [7,4–6].

The loop effects of the MSSM particles on the Higgs potential could be parametrized in a simple and elegant way by using the effective potential approximation [12]. For $\tan\beta \lesssim 40$, the radiative corrections to the potential is dominated by the top quark and top squark loops as discussed in [4,5]. Diagonalization of the top squark matrix is accomplished by a unitary transformation with a unitary matrix $U_{\tilde{t}}$ which can be parametrized by the top squark left-right mixing angle $\theta_{\tilde{t}}$ and the phase $\gamma_t \equiv \text{Arg}\{A_t - \mu \cot\beta\}$ [4,5].

On the other hand, the mass-squared matrix of the Higgs scalars, after including the one-loop radiative corrections, is a 3×3 matrix (in the basis $\mathcal{B} = \{\phi_1 \equiv \text{Re}[H_1^0], \phi_2 \equiv \text{Re}[H_2^0], A \equiv \sin\beta\text{Im}[H_1^0] + \cos\beta\text{Im}[H_2^0]\}$) having all entries nonvanishing. In particular, those entries of the matrix connecting $\phi_{1,2}$ to A are proportional to $\sin(\gamma_A + \gamma_\mu)$ ¹, and they break CP invariance in the Higgs sector explicitly [5]. Diagonalization of the Higgs mass-squared matrix can be accomplished with a 3×3 orthonormal matrix R as $(H_1, H_2, H_3) = R^T(\phi_1, \phi_2, A)$. Here $H_{i=1,2,3}$ refer to the mass eigenstate Higgs scalars, and each of them has odd- and even-CP composi-

¹Here we neglect the radiatively-induced alignment between the Higgs doublets [14].

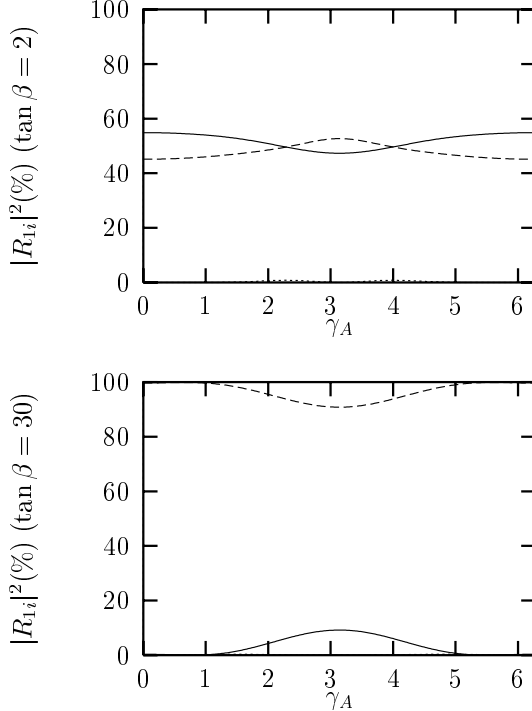


Figure 1. $|R_{11}|^2$ (solid), $|R_{12}|^2$ (dashed) and $|R_{13}|^2$ (dotted) in percents for $\tan\beta = 2$ (up) and $\tan\beta = 30$ (down).

tions. Therefore, none of the mass eigenstate Higgs bosons is a CP eigenstate.

In illustrating the CP compositions of the mass eigenstate Higgs particles, and analyzing the $ZH_{CP\ even}H_{CP\ odd}$ vertex γ_A and $\tan\beta$ will be left free; however, the remaining parameters are fixed as: $M_{\tilde{L}} = M_{\tilde{R}} = 500$ GeV; $|A_t| = 1.3$ TeV; $|\mu| = \mu = 250$ GeV; $\tilde{M}_A = 200$ GeV [4]. In presenting the figures our convention will be such that H_1 , H_2 and H_3 reduce, respectively, to the lightest CP-even, heavy CP-even, and pseudoscalar Higgs particles when $\gamma_A \rightarrow 0$.

Fig. 1 shows the CP compositions of the lightest Higgs H_1 as a function of γ_A for $\tan\beta = 2$ (upper window) and $\tan\beta = 30$ (lower window). As the figure suggests, for $\tan\beta = 2$, CP-even

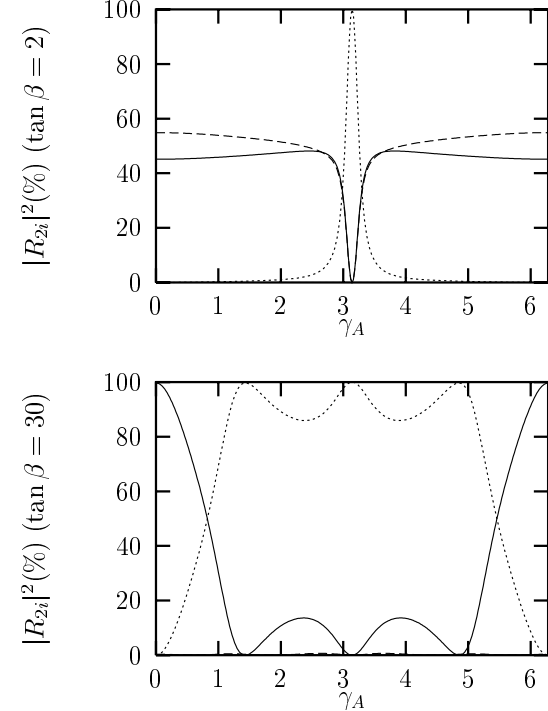


Figure 2. The same as Fig. 1 but for H_2 .

components of H_1 oscillate between $\sim 45\%$ and $\sim 55\%$ in the entire γ_A range while its CP-odd component remains below 1% everywhere. On the other hand, for $\tan\beta = 30$, $|R_{12}|^2$ remains above $\sim 90\%$, and correspondingly $|R_{11}|^2$ is always below $\sim 10\%$. This time its CP-odd component is even smaller; it never exceeds $\sim 0.5\%$. This rearrangement of the various CP compositions results from the increase in $\tan\beta$ which decouples light and heavy sectors.

Depicted in Fig. 2 are the CP compositions of H_2 . Away from $\gamma_A = \pi$ behaviour of all three curves follows from Fig. 1. For $\gamma_A \sim \pi$, however, H_2 becomes a pure CP-odd particle contrary to its pure CP-even character at $\gamma_A = 0$. This change in the CP-purity of H_2 as γ_A switches from one CP-conserving point to the next results from change in the strength of the radiative cor-

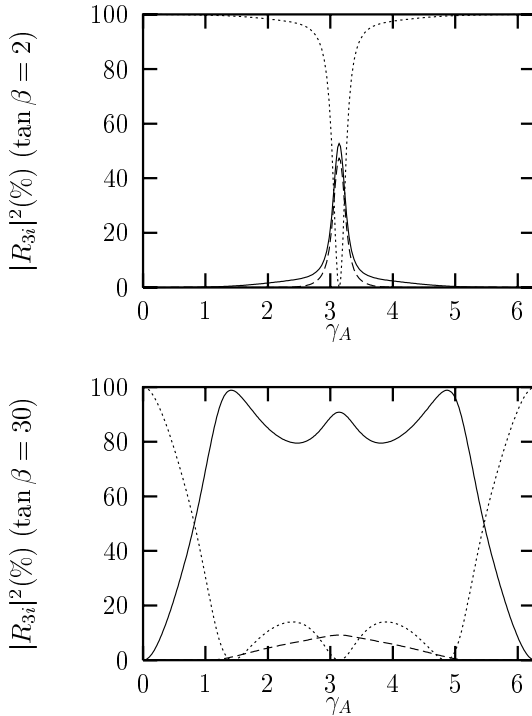


Figure 3. The same as Fig. 1 but for H_3 .

rections; for the same parameter set the light top squark is much lighter at $\gamma_A = \pi$ than $\gamma_A = 0$ [4]. Fig. 3 shows the CP compositions of H_3 , and its interpretation is similar to that of H_2 since these two have opposite CP quantum numbers at the CP-conserving points.

After specifying the CP compositions of the mass eigenstate Higgs bosons H_i in Figs. 1-3, we now turn to the discussion of $e^+e^- \rightarrow H_{CP\ even}H_{CP\ odd}$ scattering by studying $ZH_{CP\ even}H_{CP\ odd}$ vertex. In particular, we discuss the production of H_2 and H_3 in association with H_1 to observe the effects of odd- and even-CP compositions. It is possible to realize H_2H_3 production as well; however, for a $\sqrt{s} = 500$ GeV e^+e^- collider, as we consider here, this mode is phase space suppressed. The radiative corrections in the Higgs sector is not the whole story

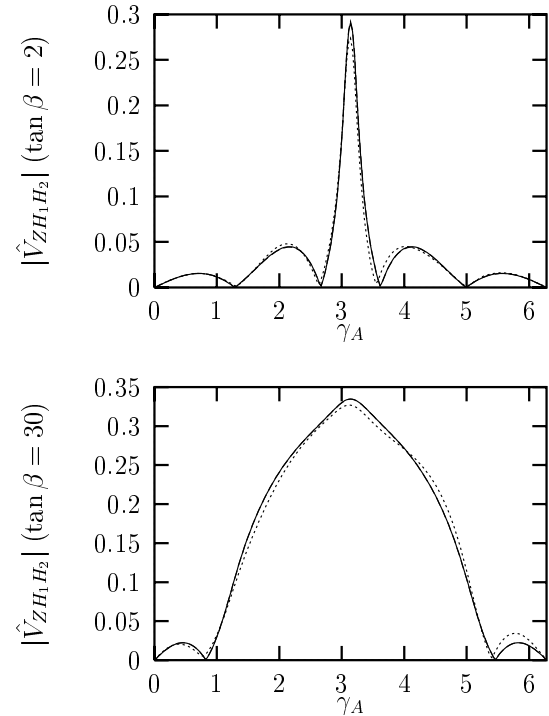


Figure 4. Variation of ZH_1H_2 coupling with γ_A when there is no vertex correction (solid), with only top quark contribution (dashed), and with full vertex correction (dotted).

because one has to include vertex radiative corrections too [9]. In this respect, consistent with the approximations for the Higgs sector, we consider top quark and top squark triangles in computing the one-loop vertex corrections [4]. Contrary to the CP-conserving theory [9], here the explicit CP-violation allows for a pseudoscalar to couple to identical top squarks, which, when the latter is light, enhances the vertex radiative corrections [4].

Fig. 4 illustrates the absolute magnitude of ZH_1H_2 coupling $|\hat{V}_{H_1H_2Z}|$ when there is no vertex correction (solid curve), when only the top quark loop is considered (dashed curve), and when both top quark and top squark loops are

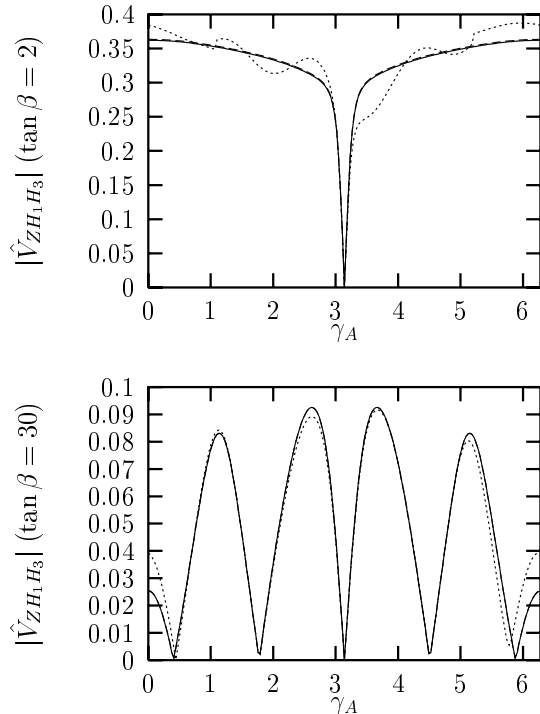


Figure 5. The same as Fig. 4 but for ZH_1H_3 coupling.

included (dotted curve). For $\gamma_A = 0$ this vertex necessarily vanishes as both Higgs bosons are CP-even. As γ_A increases, however, this vertex starts having non-vanishing values due to the CP-compositions of H_1 and H_2 in Figs. 1 and 2. A glance at the upper windows of Figs. 1, 2 and 4 shows that, even if the CP-odd compositions are much smaller than the CP-even ones, since $|\hat{V}_{H_1H_2Z}|$ vertex involves the multiplication of these two, one has an enhancement in the coupling. This statement remains valid also for $\tan \beta = 30$, as can be seen from the lower windows of the same figures. In both windows of Fig. 4 one observes the maximization of $|\hat{V}_{H_1H_2Z}|$ at $\gamma_A = \pi$ which, obviously, follows from the opposite CP purities of H_1 and H_2 at this point. One notices that, for both values of $\tan \beta$, ver-

tex radiative corrections are small compared to radiative corrections in the Higgs sector. This has different reasons for different $\tan \beta$ values. For $\tan \beta = 2$, away from $\gamma_A = \pi$, CP-odd compositions of H_1 and H_3 are small, and this suppresses the vertex radiative corrections. For $\gamma_A \sim \pi$, radiative corrections are given by the ones in the CP-conserving theory [9], which are already small. For $\tan \beta = 30$, despite rather enhanced CP purities of H_1 and H_2 , $|\hat{V}_{H_1H_2Z}|$ remains at similar magnitude with its value for $\tan \beta = 2$. This is due to the suppression of ϕ_2 component in $|\hat{V}_{H_1H_2Z}|$ with large $\tan \beta$ as it is proportional to $\cos \beta$ [4].

Depicted in Fig. 5 is the absolute magnitude of ZH_1H_3 coupling $|\hat{V}_{H_1H_3Z}|$ when there is no vertex correction (solid curve), when only the top quark loop is considered (dashed curve), and when both top quark and top squark loops are included (dotted curve). This vertex remains necessarily non-vanishing as $\gamma_A \sim 0$ since H_1 and H_3 become, respectively, the lightest and the pseudoscalar Higgs bosons of the CP-conserving theory. On the other hand, as is obvious from Fig. 3, this vertex must vanish at $\gamma_A = \pi$ since here H_2 and H_3 exchange their CP properties they have at $\gamma_A = 0$. Moreover, as is clear from a comparison of the two windows, with increasing $\tan \beta$ the entire vertex gets suppressed due to the fact that the decoupling limit is approached [9,13]. The behaviour of the solid curves follows from the CP compositions of H_1 and H_3 in Figs. 1 and 3, and their interpretation proceeds as in ZH_1H_2 vertex. In both figures, inclusion of the top quark contribution does not lead to a significant change as its $\tan \beta$ dependence is similar to the tree vertex. For small γ_A results of the CP-conserving theory are valid because coupling of the pseudoscalar components of H_1 and H_3 to identical top squark mass eigenstates is both small, and is a two-loop effect. The latter statement follows from the fact that the pseudoscalar coupling to two identical top squarks is pure imaginary and it does not interfere with the tree vertex. This remains true until the light top squark triangle develops an absorptive part which happens when the light stop mass falls below $\sqrt{s}/2$. Indeed, the sharp change in the behaviour of the dotted curve near $\gamma_A \sim 1$,

which is clear in the upper window, confirms this expectation. For $1 \lesssim \gamma_A \lesssim 5$ the light stop triangle keeps having a non-vanishing absorptive part because of which the vertex radiative corrections are enhanced. Here one observes that $|\hat{V}_{H_1 H_3 Z}|$ (dotted curve) is no longer symmetric with respect to $\gamma_A = \pi$ because of $\sim \sin \gamma_A \cos \gamma_A$ type dependence of the pseudoscalar coupling to the identical top squarks. For $\tan \beta = 30$, the mass of the light top squark is already below $\sqrt{s}/2$ in the entire range of γ_A so that interference effects due to light top squark triangle are at work. However, due to large $\tan \beta$ $|\hat{V}_{H_1 H_3 Z}|$ is suppressed, and vertex radiative corrections remain small compared to the tree vertex.

3. Conclusion

As described by Figs. 1-3 the Higgs bosons of the MSSM do not have definite CP properties due to explicit CP violation. However, one notices that the lightest Higgs boson has its CP-odd component much smaller than the CP-even ones, and the heavier Higgs bosons have alternating CP compositions as γ_A varies. The pair production process discussed here enables one to probe the CP compositions of the Higgs bosons. In general, from the analysis of $|\hat{V}_{Z H_1 H_{j \neq 1}}|$ one concludes that $e^+ e^- \rightarrow H_1 H_{j \neq 1}$ cross section is enhanced or suppressed depending on the value of CP violating phase γ_A . Associated production of the lightest Higgs with heavier ones is generally suppressed with increasing $\tan \beta$ [13]. This statement has been confirmed by Figs. 4 and 5; however, there are certain values of γ_A for which $e^+ e^- \rightarrow H_1 H_3$ cross section is twice or more larger than its value in the CP-conserving theory. Needless to say, $e^+ e^- \rightarrow H_1 H_2$ cross section is completely new as it does not exist in the CP-respecting limit. In this sense, suppression of the pair production amplitude is less than the one expected in the CP-conserving MSSM for large $\tan \beta$ [13]. However, we stress that such enhancements follow from the radiative corrections in the Higgs sector rather than the vertex radiative corrections. In this sense, it is the CP violation in the Higgs sector that is important; as already discussed in [9] the vertex radiative corrections are

small. As described here, discussion of the pair production process enables one to have a joint analysis of the even- and odd- CP Higgs bosons in the MSSM. On the other hand, one recalls that the well-known Bjorken process $e^+ e^- \rightarrow Z H_j$ is expected to yield three distinct CP-even Higgs bosons for large enough collider energies if there is explicit CP violation in the MSSM. Such an unusual signature follows from the violation of the CP symmetry. Therefore, one concludes that the Higgs search at future $e^+ e^-$ machines NLC [16] and TESLA [17] could be highly important for determining the fate of the supersymmetric CP violation.

REFERENCES

1. J. Rosiek, Phys. Rev. **D41** (1990) 3464.
2. M. Dugan, B. Grinstein and L. J. Hall, Nucl. Phys. **B255** (1985) 413.
3. S. Dimopoulos and S. Thomas, Nucl. Phys. **B465** (1996) 23.
4. D. A. Demir, hep-ph/9809360.
5. D. A. Demir, hep-ph/9901389.
6. A. Pilaftsis and C. E. M. Wagner, hep-ph/9902371; A. Pilaftsis, Phys. Rev. **D58** (1998) 096010; Phys. Lett. **B435** (1998) 88.
7. D. A. Demir, A. Masiero and O. Vives, Phys. Rev. Lett. **82** (1999) 2447; S. Baek and P. Ko, hep-ph/9812229; hep-ph/9904283.
8. M. Quiros, these proceedings.
9. P. H. Chankowski, S. Pokorski, J. Rosiek, Nucl. Phys. **B423** (1994) 437; 497.
10. T. Falk and K. A. Olive, Phys. Lett. **B375** (1996) 196.
11. T. Falk, K. A. Olive, and M. Srednicki, Phys. Lett. **B354** (1995) 99.
12. A. Brignole, Phys. Lett. **B277** (1992) 313; J. Ellis, G. Ridolfi, F. Zwirner, Phys. Lett. **B257** (1991) 83; **262** (1991) 477.
13. H. E. Haber, hep-ph/9505240.
14. D. A. Demir, hep-ph/9905571.
15. D. Chang, W.-Y. Keung, and A. Pilaftsis, Phys. Rev. Lett. **82** (1999) 900.
16. NLC ZDR Design Group, NLC Physics Working Group, hep-ex/9605011.
17. R. Brinkman, DESY-M-97-04, (1997); Turk. J. Phys. **22** (1998) 661.